Algerian Journal of Engineering and Technology

Journal homepage: https://jetjournal.org/index.php/ajet

Original Article

Transient electron transport in the ternary alloys $Al_xGa_{1-x}N$, $In_xGa_{1-x}N$, $Al_xIn_{1-x}N$ using the Monte Carlo method of simulation.

Nadia Bachir* and Nasr Eddine Chabane-Sari

Unity of Research of Materials and Renewable Energies (URMER), Department of Physics, University of Tlemcen BP: 119 TLEMCEN 13000 ALGERIA

ARTICLE INFO

Article history:
Received 13 March 2022
Revised 21 April 2022
Accepted 17 May 2022

Keywords:
$Al_xGa_{1-x}N$
$In_xGa_{1-x}N$
$In_xAl_{1-x}N$
Electric transport
Monte Carlo method of simulation
Transitional mode.

ABSTRACT

The transient electron transport and overspeed phenomenon in the binary cubic compounds GaN, InN and AlN and their ternary alloys AlGaN, InGaN and InAlN are examined and compared. For all these alloys, the overspeed phenomenon occurs beyond the critical field at which electrons can pass from the valence band to the conduction band. This field is relatively large for these alloys, particularly when the molar fraction of aluminum is large in the InAlN and AlGaN alloys. This field can reach 500 kV/cm for AlN and it is smaller in alloys with high indium concentration. It is 70 kV/cm for InN. Thus, the critical field for these alloys can vary from kV/cm to 500 kV/cm, including 150 KV/cm for GaN. The overspeed phenomenon becomes greater in the presence of Indium and it is less important in the presence of Aluminum. The present work focuses on the electronic transport in the alloys AlxGa1-xN, $In_xGa_{1-x}N$ and $In_xAl_{1-x}N$ in the transitional mode by using the Monte Carlo method of simulation which is the most appropriate.

1. Introduction

Like all III-V compounds, nitrides elements III were very early synthesized and studied. The first monocrystals GaN high surface were epitaxial on sapphire substrates with halide vapour phase (HVPE). Since 1971, these thick layers (≥ 100 µm) have permitted the obtainment of the main optical properties, in addition to a good estimate of the forbidden energy gap and the order of three valence bands. The large gap of GaN (3.4 eV to 300 K) and the existence of alloys with other nitrides InN and AlN put these materials forward as transmitters or detectors of visible light or ultra-violet (UV) [1]. The knowledge of properties and the control of the growth of the three alloys are imperative to develop new components, especially in the field of far UV.

In the present research, the study of the electrical transport in ternary alloys AlGaN, InGAN and AlInN in transient regime is based on the Monte Carlo simulation method. The study of electrical transport in binary nitride-based compounds (GaN, AlN and InN) was carried out by Foutz et al., [2] and O'Leary et al., [3]; AlGaN alloy was also considered by researchers [4]. The study of transport in this regime is based on the study of the behavior of electrons, initially at rest, receiving an electric field. We thus notice a phenomenon called overspeed where the electrons will have a very important speed peak, before the speed stabilizes.

The Monte Carlo method of simulation consists in reproducing the various microscopic phenomena residing in semiconductor materials. This method is very important for the study of the transport properties of representative particles in the different layers of the material over time. It consists of following the behavior of each electron

* *Corresponding author*.Tel.: +213552036945
E-mail address: nadia_bachir@hotmail.com
Peer review under responsibility of University of El Oued.
 DOI: https://doi.org/10.57056/ajet.v6i1.72

subjected to an electric field in real space and in the space of wave vectors. Over time, the electrons in the conduction band will have a behavior that results from the action of the applied electric field and their various interactions in the crystal lattice. The dispersion mechanisms that are taken into consideration in this research are those of: acoustic phonons and optical phonons, in addition to ionized and piezoelectric impurities, in a non-parabolic band.

To apply this method, it is necessary to introduce into the program a certain number of parameters for each material: the lattice parameter, the non-parabolicity coefficient, the dielectric constant …

For ternary alloys, the lattice parameters can be deduced from the parameters of GaN, InN and AlN by linear interpolation, as Végard's law states [5]. The effective masses, the mechanical dielectric constant can often be deduced by linear interpolation of the factors of GaN, InN and AlN.

$$X_{AlxGa1-xN} = x.X_{AlN} + (1-x).X_{GaN} \quad (1)$$
$$X_{InxGa1-xN} = x.X_{InN} + (1-x).X_{GaN} \quad (2)$$
$$X_{AlxIn1-xN} = x.X_{AlN} + (1-x).X_{InN} \quad (3)$$

In the Table 1, some parameters of ternary compounds are given as a function of those of binary compounds by Vegard's law

Table I :Nominal material parameter selections for wurtzite GaN, InN, and AlN.

Parameter	GaN	AlN	InN	$Al_xGa_{1-x}N$	$In_xGa_{1-x}N$	$Al_xIn_{1-x}N$
Lattice parameter A°	4,50 [4]-[6]-[7]	4,38 [4]-[6]-[7]	4,98 [4]-[6]-[7]	$4,5-0,12x$	$4,5+0,48x$	4,98-0,6x
Crystal density (Kg/m^3)	6, 095 [8]-[9]	5,858 [8]-[9]	6,81[2]	6, 095-0,237x	6, 095+ 0,715x	6,81-0,952x
Longitudinal sound velocity	6560 [12]-[13]	6240 [10]-[11]	9060 [2]	6560-320x	6560+ 2500x	9060-2820x
transversal sound velocity	2680[12]-[13]	2550[10]-[11]	3700 [2]	2680-430x	2680+ 1020x	3700-1150x
High frequency relative	9,5[12]-[13]	8,5[10]-[11]	8,4 [2]	9,5-x	9,5-1,1 x	8,4-0,1x
Low frequency relative	5,35[12]-[13]	4,67[10]-[11]- [14]	15,3 [14]	5,35-0,68x	5,35+ 9,95x	15,36-10,63x
dielectric constant	8,9 [15]	8,5 [15]	15,3 [15]	8,9-0,4x	8,9+ 6,4x	15,3-6,8x
piezoelectric constant	0,138[12]-[13]	0,235[10]-[11]- [14]	0,97 [2]	0,138+0,097x	0,138+0,832x	0,97-0,555x

The InN,GaN and AlN have gaps greater than the other materials, for a smaller parameter mesh. Both have direct gaps. [2]

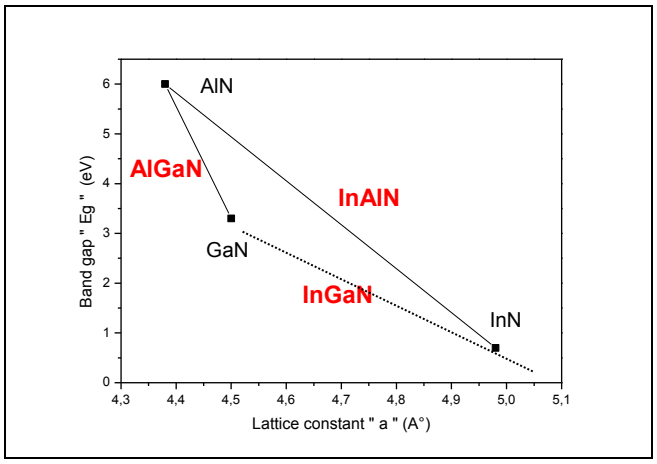

Fig 1. The band gap versus the lattice constant for GaN, AlN, InN and their alloys

With band gap energies from 0.7 eV (InN) to 6 eV (AlN) [1,3,6] and 3.3 eV for GaN [16] . Devices can be in principle designed to emit light of any color in the visible spectrum, and from the near infra-red to deep UV.

2. Software description:

In our work, we use a program written in Fortran 90 MSDEV language in order to simulate 20,000. This software performs two essential functions. The first is devoted to the calculation of probabilities from the usual expressions, by considering an isotropic and non-parabolic model with three valleys (Γ, L, X). The interactions that are taken into account are due to acoustic phonons, intermediate polar optical phonons and impurities. The second function is intended to determine the instantaneous quantities defined on a set of electrons (energy, speed, position) by the "Self Scattering" procedure [9] for which the free-flight times are distributed for each electron.

Among the parameters that must be determined to perform the simulation is the energy gap.

The change in the energy band gap of the alloy depending on the composition is not linear but quadratic.

$$E_g^{AlxGa1-xN} = x.E_g^{AlN} + (1-x).E_g^{GaN} - x.(1-x).b_{AlGaN} \quad (4)$$

$$E_g^{InxGa1-xN} = x.E_g^{InN} + (1-x).E_g^{GaN} - x.(1-x).b_{InGaN} \quad (5)$$

$$E_g^{InxAl1-xN} = x.E_g^{InN} + (1-x).E_g^{AlN} - x.(1-x).b_{InAlN} \quad (6)$$

The b coefficient represents the bowing. [2]

The bowing b for the three alloys is: b_{AlGaN}=0.688, b_{InGaN}=1.416, b_{InAlN}=3.477: [4]

In the Table 2, the parameters are given for the binary and ternary nitrids (the energy gaps, the effective masses and the non-parabolicity coefficient

Table 2: energies; the effective masses, the non-parabolicity coefficients for the three binary GaN, AlN and InN as well as the three ternaries AlGaN, InGaN and InAlN.

Paramètre		GaN	AlN	InN	AlGaN	InGaN	InAlN
Bowing					b_{AlGaN} =0.688[4]	b_{InGaN} =1.416[4]	b_{InAlN} =3.477[4]
Energie des vallées (eV)	Γ	3,2 [16]	6[1,3,6]	0,7 [1,3,6]	0.688 x^2 + 2.012 x + 3.2	1.416 x^2 − 4.016 x + 3.2	3.477 x^2 − 8.77 x + 6
	L	5,9 [16]	9,43[8]-[9]	4,09 [11]	0.688 x^2 + 3,002 x + 5.64	1.416 x^2 − 2,966x + 5.64	3.477 x^2 − 8,817 x + 9.42
	X	4,6 [16]	5,1 [8]-[9]	4,49[11]	0.688 x^2 − 0,158 x + 4.57	1.416 x^2 − 1,496 x + 4.57	3.477 x^2 − 4,087x + 5.1
Masse effective (m_0)	Γ	0,15[16]	0,21[8]-[9]	0,11[5]	0,15+0,06x	0,15-0,04 x	0,21-0,1x
	L	0 ,6 [16]	0,7[7]-[8]	0,6[5]	0,6+0,1x	0,6	0,7-0,1x
	X	0,4 [16]	0,4[7]-[8]	0,4[5]	0,4	0,4	0,4
Coefficient de non parabolicité (1/ev)	Γ	0,213	0,1052	0,419	0,213-0,1078x	0,213-0,206x	0,419+ 0,3138x
	L	0,461	0,461	0,036	0,461	0,461	0,036-0 ,445x
	X	0,204	0,204	0,0088	0,204	0,204	0,0088-0,1952x

The model of Kane is used to calculate the coefficient of non-parabolicity [16]

$$\alpha = \frac{1}{E_g}\left(1 - \frac{m^*}{m_0}\right)^2 \quad (7)$$

where α is the non-parabolicity coefficient, Eg represents the corresponding energy gap, m* being the effective mass and m_0 denote the mass of free electrons

By entering the previous parameters into the program, in addition to the temperature, the simulation time and the electric field, the results are obtained in a file, and are strongly dependent on the parameters which characterize the material.

The developments brought to our software have made it simpler and more user-friendly [13]. The general procedure for running this software consists of three essential steps which can be summarized as follows [17]:

1- Input: reading the data file concerning the parameters of the material used, such as: the energy gaps, the effective masses, the deformation potentials, the non-parabolicity coefficients, the speed of sound, the concentration of impurities, the temperature of the network, applied electric fields, etc. in a.txt file,

2- Running the software.

3- Output: retrieving the files containing the values of the interaction probabilities, the speeds in the different valleys, the energies, etc.

3. Results and Discussion

3.1 Speed as a function of time

To highlight the effects of non-stationary transport that can occur in InGaN, AlGaN and InAlN alloys, we study the behavior of a group of electrons subjected to sudden variations in the electric field, i.e. as we apply different electric field levels.

To ensure a stable behavior for electrons, we initially apply a 10 kV/cm field for a time equal to 1ps. Then the electrons undergo a level of electric field. The results for the AlGaN, InGaN and InAlN alloys are shown in Fig. 2, 5 and 8, respectively.

3.1.2 Speed as a function of time for AlGaN alloy

The electron velocity versus the time for different levels of electric field within GaN, $Al_{0.2}Ga_{0.8}N$, $Al_{0.5}Ga_{0.5}N$, $Al_{0.8}Ga_{0.2}N$ and AlN are given in figure 2

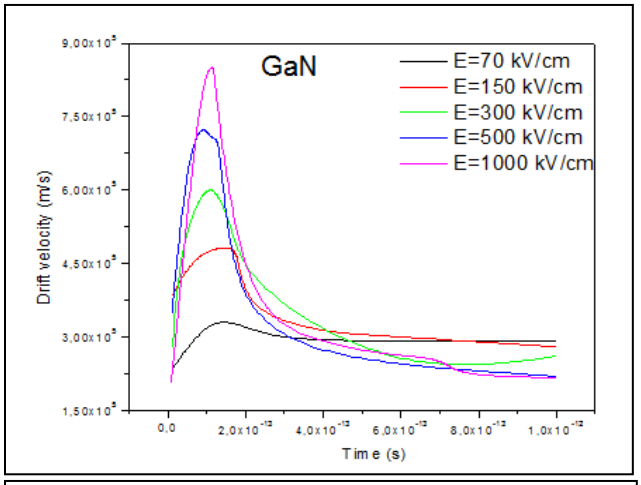

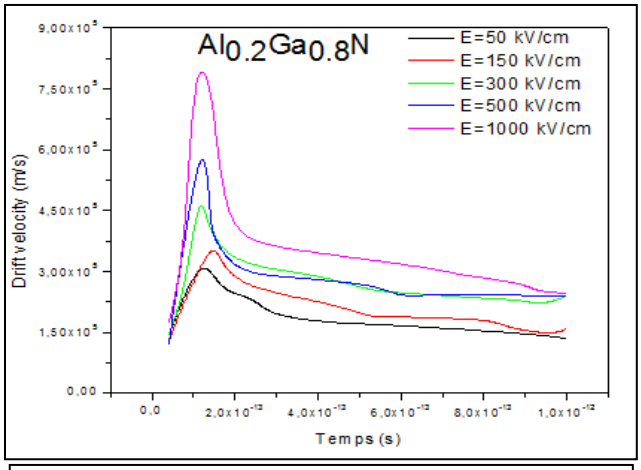

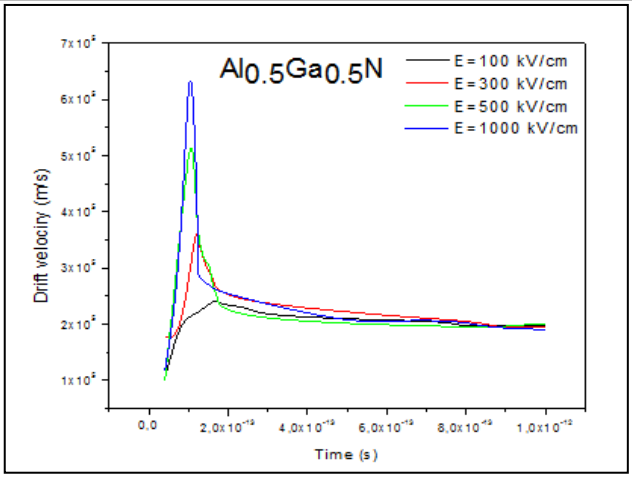

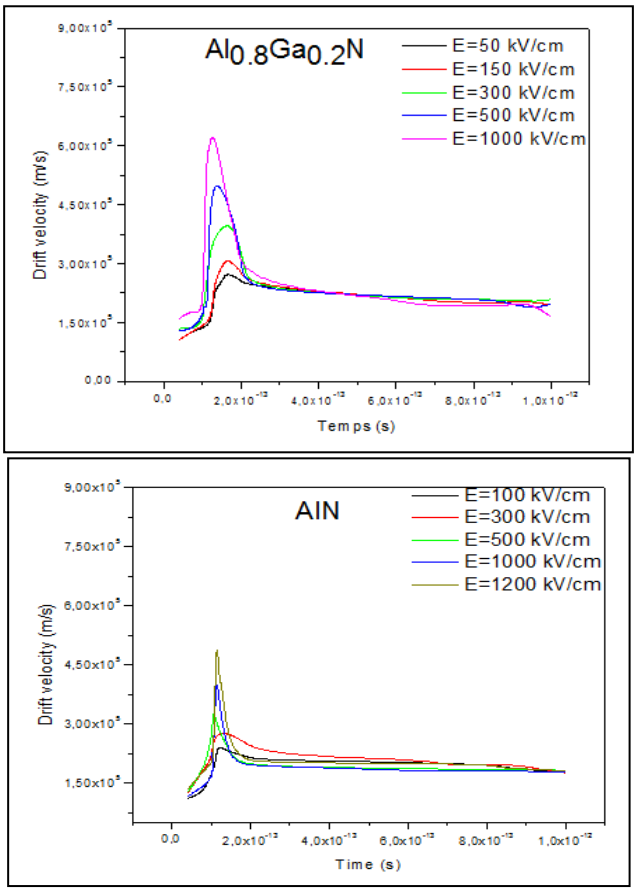

Fig 2. The electron velocity versus the time for different levels of electric field within GaN, $Al_{0.2}Ga_{0.8}N$, $Al_{0.5}Ga_{0.5}N$, $Al_{0.8}Ga_{0.2}N$ and AlN.

In this case the applied fields vary between small values 50 kV/cm, 150kV/cm,… up to large values 1000 kV/cm for GaN, $Al_{0.2}Ga_{0.8}N$, $Al_{0.5}Ga_{0.5}N$ and 1200 kV/cm for $Al_{0.8}Ga_{0.2}N$ and AlN

The speed peaks as a function of the electric field for the AlGaN alloy, for different aluminum mole fractions, are shown in Figure 3.

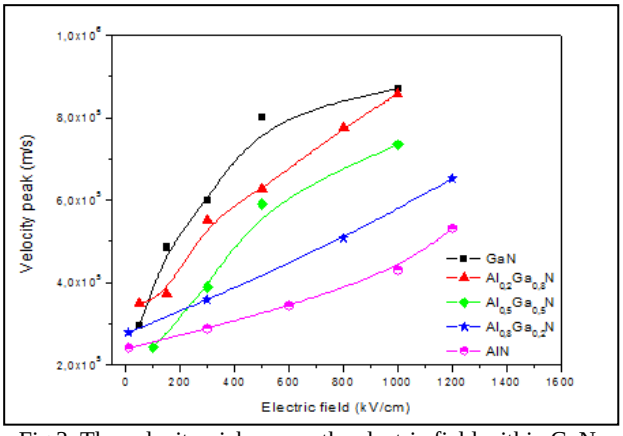

Fig 3. The velocity pick versus the electric field within GaN, $Al_{0.2}Ga_{0.8}N$, $Al_{0.5}Ga_{0.5}N$, $Al_{0.8}Ga_{0.2}N$ and AlN

For an electric field lower than the critical field (<140 kV/cm), the overspeed effect is not observable in the AlGaN alloy, whatever the molar fraction of Al.

From 140 kV/cm to 400 kV/cm, the speeds start to show a sharp peak in the case of the AlGaN alloy for all Al molar fractions. The speed peak begins to appear when the electric field reaches the critical field for which the electrons can pass from the valence band to the conduction band.

In Figure 4, the maximum steady-state velocities are given as a function of the critical field, for the AlGaN alloy for all Al molar fractions. These results were found in the study of stationary electric transport. N. Bachir et al 5 [18].

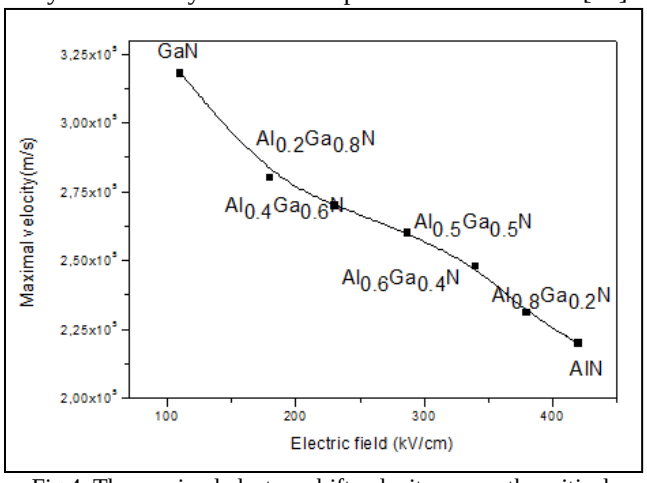

Fig 4. The maximal electron drift velocity versus the critical applied electric field within $Al_xGa_{1-x}N$ for different mole fractions x of Aluminum, at T = 300K

In the case of GaN, this peak for the 140 kV/cm field is 5×10^5 m/s for a time of 0.1ps. For the 300 kV/cm field, the maximum speed is $6x10^5$ m/s for a time of 0.1ps. The top speed is reached during the same time in both fields.

By increasing the molar fraction of Al, the critical field, for which the speed of the electrons reaches its maximum, becomes larger and larger, and the phenomenon of overspeed begins to appear for increasingly larger fields. For AlN, this phenomenon begins for fields greater than 600 kV/cm.

At 600 kV/cm, cubic AlN has a maximum speed of 3.2×10^5 m/s for 0.05ps of duration. The response time in this case is very low. After this time, the speed will drop to 2×10^5 m/s for a period of 0.6ps.

The energy gained by the free carrier in the valley will give it acceleration until reaching the maximum speed. In this valley, the electron has low mass and high mobility. But when the energy of the electron reaches the energy of transfer to the other valleys, its mass increases (it will be heavier); its mobility will decrease and it will be blocked by other carriers already existing in that valley. Its speed will then decrease to tend towards a stationary value.

3.1.2 Speed as a function of time for InGaN alloy

The electron velocity versus the time for different levels of electric field within $In_{0.2}Ga_{0.8}N$, $In_{0.5}Ga_{0.5}N$, $In_{0.8}Ga_{0.2}N$ and InN are given in figure 5

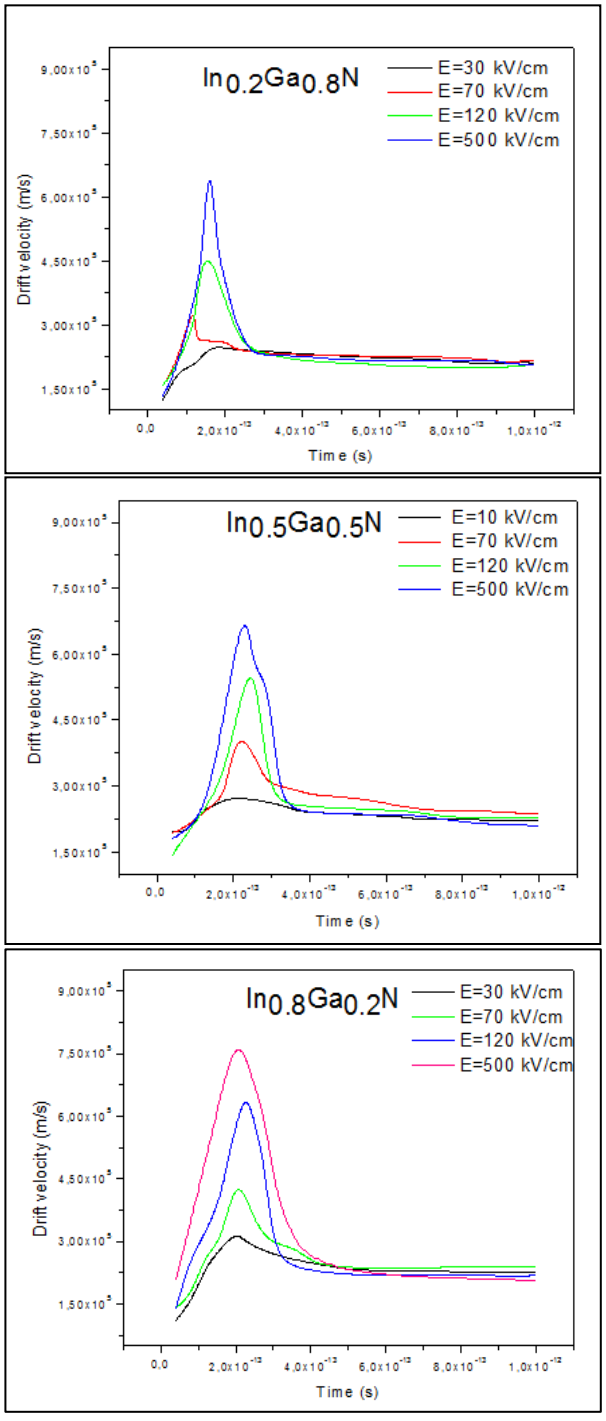

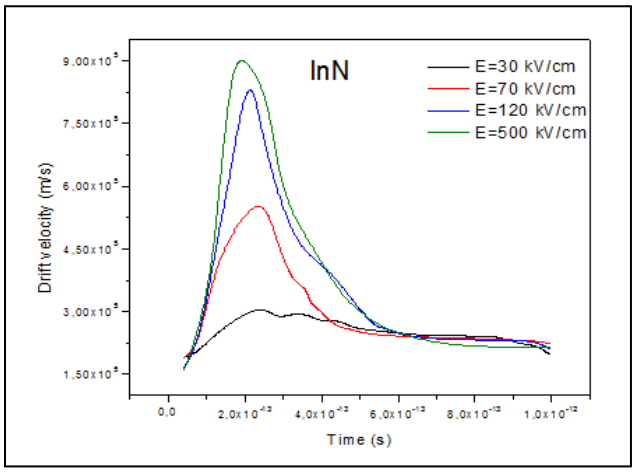

Fig 5.The electron velocity versus the time for different levels of electric field within $In_{0.2}Ga_{0.8}N$, $In_{0.5}Ga_{0.5}N$, $In_{0.8}Ga_{0.2}N$ and InN.

In this case the applied fields vary between very small values 30 kV/cm, 70kV/cm,… up to large values which in this case do not exceed 500 kV/cm especially for InGaN alloys having a large molar fraction of Indium because in this case the gap is small and the alloy is not very resistant

The speed peaks as a function of the electric field for the InGaN alloy, for different aluminum mole fractions, are shown in Figure 6.

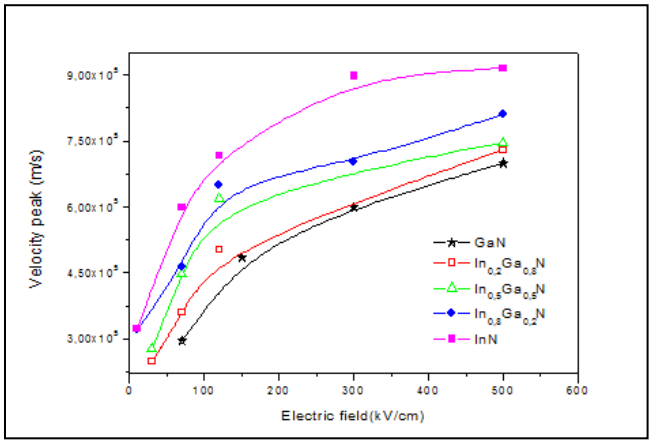

Fig 6. The velocity peak versus the electric field within GaN, $In_{0.2}Ga_{0.8}N$, $In_{0.5}Ga_{0.5}N$, $In_{0.8}Ga_{0.2}N$ and InN.

By increasing the molar fraction of In in the InGaN alloy, the critical field, for which the speed of the electrons reaches its maximum, becomes smaller i.e. by increasing the molar fraction of In, the overspeed phenomenon begins to appear for smaller fields.

For InN, this phenomenon begins for fields greater than 70 kV / cm. From these figures, we can make four observations:

1. Overspeed peaks appear from 70 kV / cm.
2. The overspeed peaks become larger as the electric field increases.
3. The peaks move towards the weak times as the field

increases.

4. The equilibrium state is reached more quickly for large fields.

The critical fields for which the speed reaches its maximum in a steady state, in the InGaN alloy, are given in figure 7. This figure shows the maximum speeds as a function of the critical field for different molar fraction of indium. These results were found by A. hamdoune and N. Bachir [19].

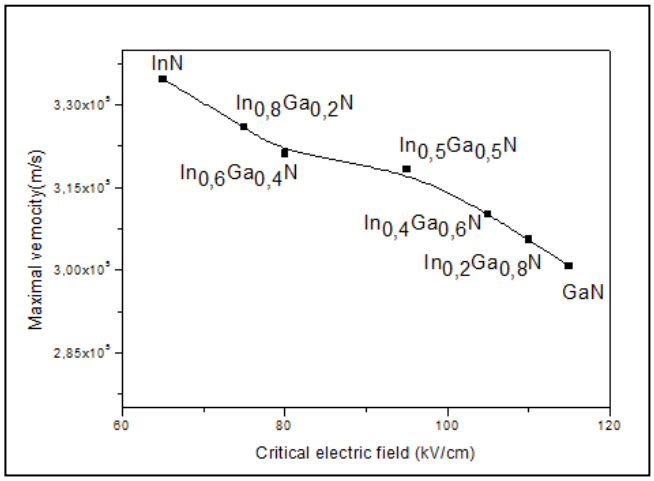

Fig 7. The maximal electron drift velocity versus the applied electric field within $In_xGa_{1-x}N$ for different mole fractions x of Aluminum, at T = 300K

On the one hand, the overspeeds in the InGaN alloy are very high and increase with the molar fraction of In. On the other hand, this speed is relatively lower in the AlGaN alloy and decreases with the addition of Al. The top speed in this case is very sharp compared to the InGaN alloy, so that the lifetime of the electrons becomes longer in the presence of In and augments with the increase of In, which is very important in optoelectronics.

The overshoots within the InGaN alloy are very large and increase with the augmentation of the molar fraction of In. In the AlGaN alloy, they are relatively smaller and decrease with the increase in the molar fraction of Al.

The response time is very low in the two alloys, of the order of picoseconds (or smaller). This means that the lifetime of electrons is very long, which is very important in optoelectronic devices.

Within InGaN, the energy and speed of electrons are very important for weak fields and low temperatures. Within AlGaN, the breakdown voltage is high thanks to the wide band gap, allowing high output impedance and high saturation speed. AlGaN is more resistant to high temperatures and high pressures.

The two alloys are complementary: InGaN is more efficient at weak electric fields and at low temperatures[20-21]; AlGaN is more efficient for high electric fields and high temperatures [18-19].

3.1.3 Speed as a function of time for InAlN alloy

The electron velocity versus the time for different levels of electric field within $In_{0.2}Al_{0.8}N$, $In_{0.5}Al_{0.5}N$, $In_{0.8}Al_{0.2}N$ are given in figure 8

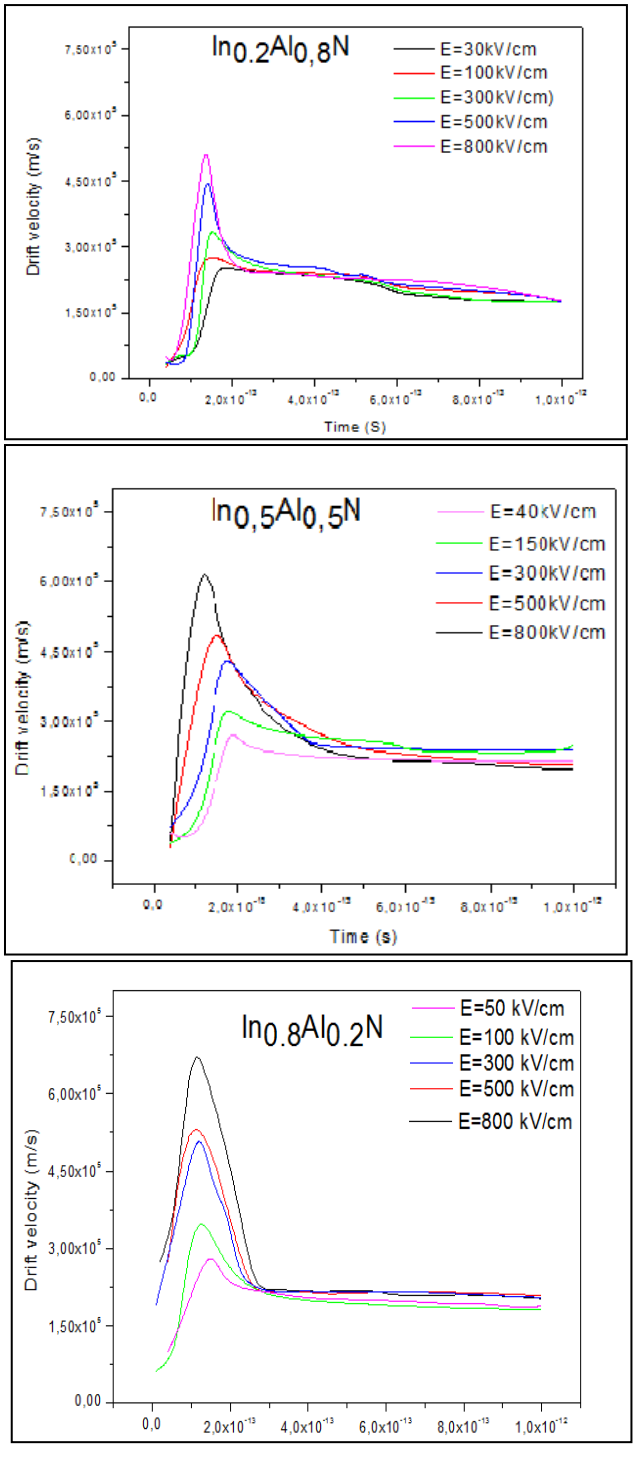

Fig. 8 : The electron velocity versus the time for different levels of electric field within $In_{0.2}Al_{0.8}N$, $In_{0.5}Al_{0.5}N$, $In_{0.8}Al_{0.2}N$

.

The peak speeds for the InAlN alloy are given as a function of the electric field for different mole fractions of Indium
In this case the applied fields vary between small values 40 kV/cm, 150kV/cm, up to large values which in this case do not exceed 800 kV/cm and 1200 kV/cm for AlN.
By increasing the molar fraction of In in the InAlN alloy, the overspeed phenomenon begins to appear for smaller and smaller fields. For InN, this phenomenon begins for fields greater than 70 kV / cm.
The speed peaks as a function of the electric field for the InAlN alloy, for different indium mole fractions, are shown in Figure 9.

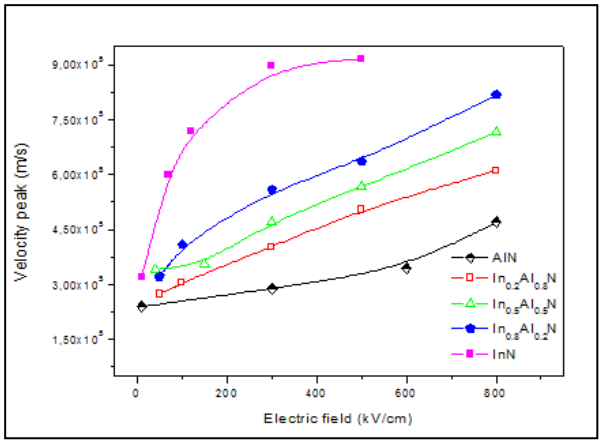

Fig 9. The velocity peak versus the electric field within AlN, $In_{0.2}Al_{0.8}N$, $In_{0.5}Al_{0.5}N$, $In_{0.8}Al_{0.2}N$ and InN .

Figure 10 shows the maximum speeds as a function of the critical fields for the InAlN alloy for different Indium molar fractions, in a steady state. This study was conducted by N. Bachir et al.[20].

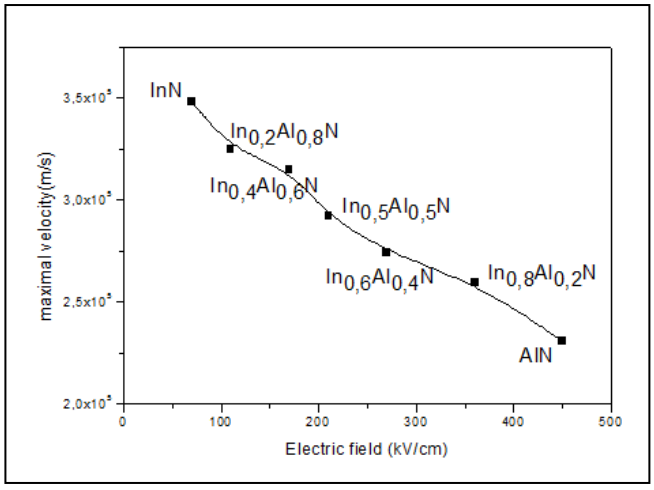

Fig 10. The maximal electron drift velocity versus the applied electric field within $In_xAl_{1-x}N$ for different mole fractions x of Aluminum, at T = 300K

The overspeed phenomenon in the InAlN alloy is more significant than in the case of the AlGaN alloy due to the presence of In. On the other hand, this speed is relatively lower than that of the InGaN alloy and decreases with the addition of Al. The peak speed in this case is sharper than the InGaN alloy. Hence, the lifetime of electrons becomes greater in the presence of In, and increases by adding In, which is very important in optoelectronics.
The overshoots within the InGaN alloy are very large and increase with the molar fraction of In. In the AlGaN alloy, they are relatively smaller and decrease with the increase of the molar fraction of Al.
The response time is very low in the two alloys, of the order of picoseconds (or smaller). This means that the lifetime of electrons is very long, which is very important in optoelectronic devices.
Within InGaN and InAlN alloys, the energy and speed of electrons are very important for weak fields and low temperatures. Within AlGaN, the breakdown voltage is high thanks to the wide band gap, allowing high output impedance and high saturation speed. AlGaN and InAlN (with small molar fractions of Indium) are more resistant to high temperatures and high pressures.
The two alloys are complementary: InGaN is more efficient at weak electric fields and at low temperatures; AlGaN is more efficient for high electric fields and high temperatures.
By changing the molar fraction of Indium in the InAlN alloy, we can have the two advantages of the other ternaries. For small molar fractions of In, the ternary compound is effective for large electric fields and high temperatures. Whereas large In molar fractions in InAlN work best in weak electric fields and at low temperatures.

4. Conclusion

GaN, AlN, InN and their alloys constitute a major research area in solid state electronics for analog hyper-frequency wave applications. These materials have several advantages including their high voltage thanks to their large gap allowing higher output impedance, their saturation at high speed, and their high linearity. They are also characterized by their resistance to electromagnetic pulses, their chemical stability and their stability at high temperature. Cubic alloys have great potential for optoelectronics, especially in the case of far ultraviolet. However, it will be necessary to clearly determine the nature of the deviation for high aluminum concentrations. Moreover, the quality of the epitaxy layers is still quite low compared to those of hexagonal nitrides. The development of optoelectronic applications from cubic nitrides will therefore make it possible to better control the growth, which is relatively difficult due to the nature of the

metastable cubic phase and the lack of homogeneous and good quality cubic SiC substrates.

Acknowledgements

The authors acknowledge the support of DGRSDT for this work.

Conflict of Interest

We declare that they have no conflict of interest

References

1. Roosen G. Materiaux pour l'Optoelectronique, Traite EGEM serie Optoelectronique., tome 7, *Hermes Science Publications*, Paris, 2003.
2. Foutz BE, O'Leary SK, Shur MS, Eastman LF. Transient electron transport in wurtzite GaN, InN, and AlN. *Journal of applied physics*. 1999;85(11):7727-7734.
3. O'Leary SK, Foutz BE, Shur MS, Eastman LF. Steady-state and transient electron transport within bulk wurtzite indium nitride: An updated semiclassical three-valley Monte Carlo simulation analysis. *Applied Physics Letters*. 2005;87(22):222103.
4. Vurgaftman I, Meyer JÁ, Ram-Mohan LÁ. Band parameters for III–V compound semiconductors and their alloys. *Journal of applied physics*. 2001;89(11):5815-5875.
5. Albrecht JD, Wang RP, Ruden PP, Farahmand M, Brennan KF. Monte Carlo calculation of electron transport properties of bulk AlN. *Journal of applied physics*. 1998;83(3):1446-1449.
6. Wang F, Li SS, Xia JB, Jiang HX, Lin JY, Li J, Wei SH. Effects of the wave function localization in AlInGaN quaternary alloys. *Applied Physics Letters*. 2007;91(6):061125.
7. Vurgaftman I, Meyer JN. Band parameters for nitrogen-containing semiconductors. *Journal of Applied Physics*. 2003;94(6):3675-3696.
8. Madelung O. Semiconductors: data handbook. 3rd Ed. Springer Science & Business Media; 2004.
9. Dessenne F. Etude théorique et optimisation de transistors à effet de champ de la filière InP et de la filière GaN (Doctoral dissertation, Lille 1). 1998.
10. Kolnik J, Oğuzman İH, Brennan KF, Wang R, Ruden PP, Wang Y. Electronic transport studies of bulk zincblende and wurtzite phases of GaN based on an ensemble Monte Carlo calculation including a full zone band structure. *Journal of Applied Physics. 1995;78(2):1033-1038.*
11. O'leary SK, Foutz BE, Shur MS, Eastman LF. Steady-state and transient electron transport within the III–V nitride semiconductors, GaN, AlN, and InN: a review. Journal of Materials Science: Materials in Electronics. 2006;17(2):87-126.
12. Chin VW, Tansley TL, Osotchan T. Electron mobilities in gallium, indium, and aluminum nitrides. *Journal of Applied Physics*. 1994;75(11):7365-7372.
13. Hadi WA, Shur MS, O'Leary SK. Steady-state and transient electron transport within the wide energy gap compound semiconductors gallium nitride and zinc oxide: an updated and critical review. *Journal of Materials Science: Materials in Electronics*. 2014;25(11):4675-4713.
14 . Foutz BE, Eastman LF, Bhapkar UV, Shur MS. Comparison of high field electron transport in GaN and GaAs. *Applied physics letters*. 1997;70(21):2849-2851.
15. Shur M, Gelmont B, Asif Khan M. Electron mobility in two-dimensional electron gas in AIGaN/GaN heterostructures and in bulk GaN. *Journal of electronic materials*. 1996;25(5):777-785.
16. Pampili P, Zubialevich VZ, Maaskant P, Akhter M, Corbett B, Parbrook PJ. InAlN-based LEDs emitting in the near-UV region. *Japanese Journal of Applied Physics*. 2019 May 23;58(SC):SCCB33.
17. Kurosawa T. Monte Carlo calculation of hot electron problems. *In Journal of the Physical Society of Japan*, 1966; 21:424-426.
18. Bachir N, Hamdoune A, Bouazza B, Chabane-Sari NE. Effect of the temperature and doping on electron transport in AlxGa1−xN alloy by monte carlo method. *InIOP Conference Series: Materials Science and Engineering* 2010 Nov 1 (Vol. 13, No. 1, p. 012012). IOP Publishing.
19. Hamdoune A, Bachir N. Effects of Temperature and Concentration ofIndium within Bulk Cubic InxGa1-XN: Calculation of Steady State Electron Transportby Method of Monte Carlo Simulation. *International Journal of Computer and Electrical Engineering*. 2010;2(5):891.
20. Bachir N, Hamdoune A, Sari NE. Steady-state electron transport within InAlN bulk ternary nitride, using the Monte Carlo method. *International Journal of Materials Science and Applications.* 2014; 3(2): 20-24

Recommended Citation

Bachir N, Chabane-Sari NE. Transient electron transport in the ternary alloys $Al_xGa_{1-x}N$, $In_xGa_{1-x}N$, $Al_xIn_{1-x}N$ using the Monte Carlo method of simulation. *Alger. J. Eng. Technol. 2022*, 6:62-70. DOI: https://doi.org/10.57056/ajet.v6i1.72